REVIEW

Prenatal diagnosis of congenital lung malformations

Leonor Alamo · Francois Gudinchet ·
Olivier Reinberg · Yvan Vial · Katyuska Francini ·
Maria-Chiara Osterheld · Reto Meuli

Abstract Prenatal diagnosis of congenital lung anomalies has increased in recent years as imaging methods have benefitted from technical improvements. The purpose of this pictorial essay is to illustrate typical imaging findings of a wide spectrum of congenital lung anomalies on prenatal US and MRI. Moreover, we propose an algorithm based on imaging findings to facilitate the differential diagnosis, and suggest a follow-up algorithm during pregnancy and in the immediate postnatal period.

Keywords Prenatal diagnosis · Fetal MRI · Fetal ultrasonography · Congenital lung malformation

L. Alamo (✉) · F. Gudinchet · R. Meuli
Unit of Pediatric Radiology,
Department of Diagnostic and Interventional Radiology,
Centre Hospitaliere Universitaire Vaudois (CHUV),
Rue du Bugnon, 46,
1011, Lausanne, Switzerland
e-mail: Leonor.Alamo@chuv.ch

O. Reinberg
Department of Pediatric Surgery,
Centre Hospitaliere Universitaire Vaudois (CHUV),
Rue du Bugnon, 46,
1011, Lausanne, Switzerland

Y. Vial · K. Francini
Department of Obstetrics and Gynecology,
Centre Hospitaliere Universitaire Vaudois (CHUV),
Rue du Bugnon, 46,
1011, Lausanne, Switzerland

M.-C. Osterheld
Department of Pathology,
Centre Hospitaliere Universitaire Vaudois (CHUV),
Rue du Bugnon, 46,
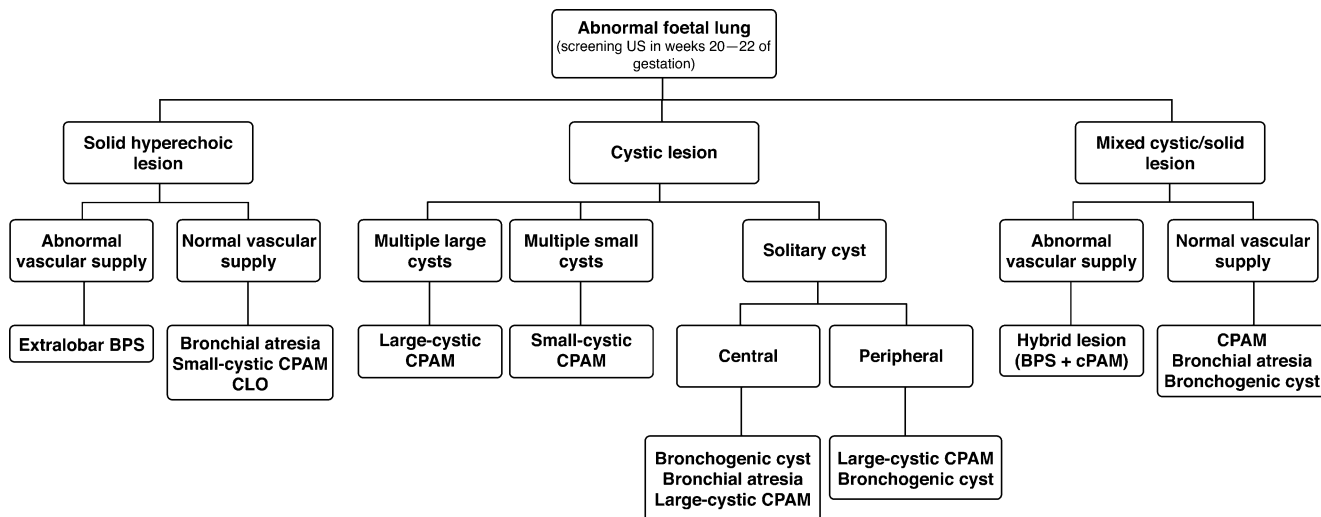1011, Lausanne, Switzerland

Introduction

Congenital lung abnormalities (CLA) are a heterogeneous group of pathologies consisting of isolated bronchopulmonary anomalies, isolated vascular anomalies or a combination of these. The most common CLAs include congenital pulmonary airway malformation (CPAM), bronchopulmonary sequestration (BPS), bronchial atresia, bronchogenic cyst and congenital lobar overinflation (CLO), also known as lobar emphysema [1]. These entities account for >95% of all CLA. Prenatal diagnosis of CLA has increased considerably in recent years due to more widespread and improved prenatal US screening. Although in most cases a well-performed US may provide a correct diagnosis, complementary MRI is increasingly performed for additional useful information in selected cases.

Prenatal diagnosis of CLA is difficult and often confusing due to overlapping findings between different lesions or to presence of complex, hybrid lesions with combined vascular and bronchopulmonary abnormalities. There is also great prenatal variability in clinical evolution and outcome, from complete involution in utero to progressive growth and secondary complications. The postnatal clinical spectrum ranges from the asymptomatic child to the child with progressive, severe respiratory distress requiring immediate intervention, but despite it no clear indications for foetal MRI or for postnatal imaging follow-up have been published.

The main purpose of this pictorial essay is to illustrate the typical findings for a wide spectrum of CLAs with an emphasis on p0renatal imaging. It is based on our own experience during the last 10 years. We also propose a diagnostic algorithm based on foetal US and MRI findings (Fig. 1) and an algorithm for follow-up of any prenatally detected lesions (Fig. 2)

Fig. 1 Diagnostic algorithm based on foetal US and MRI findings

Prenatal diagnosis

In our hospital, routine US (including color Doppler) pregnancy screening is conducted by the Department of Obstetrics and Gynaecology and performed by gynaecologists with proven experience in prenatal diagnosis (Y.V., K. F.). Standard US examinations include a detailed survey of

the foetal anatomy and an echocardiographic evaluation. They are usually performed with a GE 730 Expert (General Electric, Zipf, Austria) or an Acuson Sequoia (Sony IBL, San Diego, CA) US scanner.

If a foetal lung lesion is detected, a complete evaluation of both lungs is performed. Morphological description includes anatomical location, extension, overall echogenic-
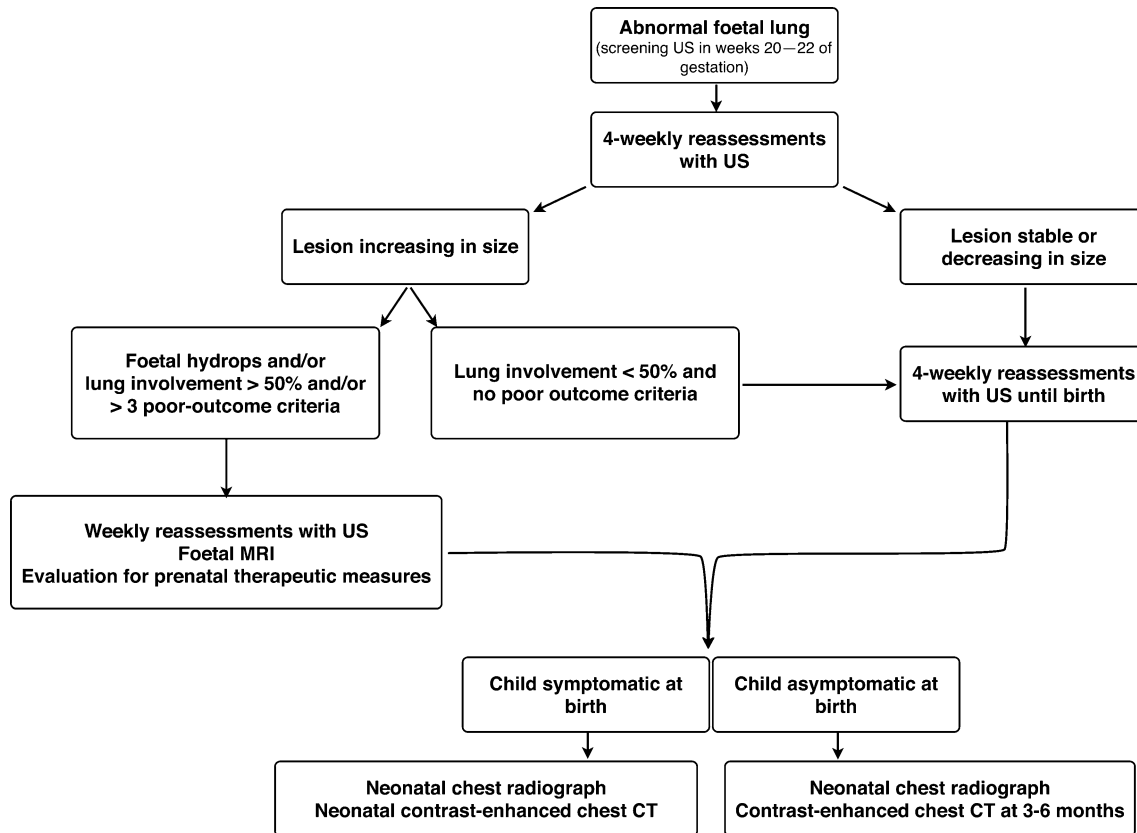

Fig. 2 Algorithm for follow-up of any prenatally detected lung lesions

ity compared to normal foetal lung, homo/heterogeneity and presence of solid/cystic/mixed components. We assess the presence/absence of an abnormal feeding artery with color Doppler. Lesions are then classified into three groups (mostly solid, mostly cystic, mixed), and the most likely differential diagnosis is suggested (Fig. 1).

After this initial exam, US controls are conducted at regular intervals, usually every 4 weeks, to follow any changes in size and to identify possible complications. In case of hydrops or signs of obstruction due to significant increase in the volume of the lesion, the foetus will be scanned at least weekly. The most important outcome criterion is the development of hydrops, which is associated with an extremely high risk of foetal or neonatal death [2–4]. Another predictor of poor outcome is the presence of at least three of the following criteria: large lesions (>50% of total foetal lung volume involved in the abnormality), transverse mass diameter-to-transverse chest diameter ratio>0.56 measured on an axial chest image in which the four-chamber view of the heart is displayed [3], volume mass-to-head circumference ratio>1.6 [4] or significant mass effect (midline and/or intercostal lung herniation, mediastinal shift, inversion of the ipsilateral diaphragm, severe hypoplasia of the remaining lung) (Fig. 2).

The aims of supplementary foetal MRI are to (1) further characterize the morphology of the lesion and its effects on normal lung, (2) determine the volumes of both the normal and abnormal lung and (3) further inform the discussion about intervention (termination of pregnancy, immediate delivery, thoracoamniotic shunting or puncture of a dominant cyst, administration of prenatal corticosteroids for treatment of severe small-cyst type CPAM, etc. [4, 5]). We perform MRI with a 1.5-T scanner (Magnetom Symphony; Siemens Medical Solutions, Erlangen, Germany) with a phased-array body coil. Our preferred scan protocol is shown in Table 1. It includes coronal, sagittal and transverse foetal sections with T2-half-Fourier single-shot turbo spin-echo (HASTE), steady-state free precession imaging (SSFP, true-FISP) and a 3-D-spoiled gradient-echo sequence (VIBE). Although we have recently added a diffusion-weighted sequence, our experience with this is limited. The entire examination does not usually exceed 30 min and is performed without sedation. The MR images are read by

senior radiologists (L.A., F.G.) with experience in foetal diagnostic imaging. The lesion is described similarly as on US (Fig. 1).

Prenatal findings

Congenital pulmonary airway malformation

Formerly known as congenital cystic adenomatoid malformation (CCAM), CPAM is a heterogeneous group of lesions caused by overgrowth of mesenchymal elements and impairment of normal alveolar development. The term CCAM is no longer considered appropriate because neither cysts nor adenomatoid elements need to be present. Most CPAMs are in the pulmonary vascular circuit and there is normal communication with the bronchial tree. Cysts of CPAM are lined by respiratory ciliated epithelium.

Stocker [6–8] initially defined three types and later expanded it to five based on postnatal cyst-size and on the histological resemblance with different segments of the developing bronchial tree. Only three types of CPAM are distinguishable at imaging and are therefore relevant for this paper: type I has at least one dominant cyst>2 cm in diameter; type II is composed of multiple, uniform small cysts < 2 cm, and type III is solid or composed of microcysts with diameter<0.2 cm [6, 7].

The exact aetiology remains unknown, but recently Langston [9] suggested in utero airway obstruction as a possible cause, hence proposing a more comprehensive classification: a large-cyst type equivalent to the type I of Stocker, and a small-cyst type, equivalent to Stocker type II. By this classification, Stocker type III is considered a form of pulmonary hyperplasia that should not be included in the CPAM group [9]. This classification seems to be more feasible for prenatal imaging.

On foetal US, CPAMs appear as hyperechoic, heterogeneous tissue with multiple hypoechoic cysts that may differ in size and number (Figs. 3, 4). MRI returns higher signal than normal lung on T2-weighted images. In the foetus, Stocker type I lesions contain cysts >5 mm in diameter (Fig. 1) whilst Stocker type II lesions contain smaller cysts (Fig. 4). These cysts are easily recognisable on T2-weighted images [10–12]. In large lesions, the expansion of the pathological

Table 1 Typical protocol (sequence parameters) used for foetal lung MRI in our center

	Slice thickness (mm)	TR (ms)	TE (ms)	Flip angle (degrees)	Field of view (mm)	Matrix
T2-HASTE	5	999	88	135	350×350	307×512
T2-TRUE FISP	5	6.44	3.22	70	350×262.5	230×512
T1-VIBE	4	3.69	1.6	12	255×340	192×256
Diffusion-weighted imaging	5	1,800	87		350×350	128×96

Fig. 3 Large-cystic type congenital pulmonary airway malformation (CPAM). Sagittal US with the foetal head to the right (**a**) and balanced steady-state free precession MRI in the sagittal (**b**) and transverse (**c**) plane in week 31 of gestation show a large, heterogenous lesion, involving most of the right lung with macrocysts of varying size. The affected lung is overexpanded, causing inversion of the ipsilateral diaphragm, compression of the right lower lobe (*star*) and the left lung and significant displacement of the heart (*H*). Neonatal chest radiograph (**d**) shows the increased volume of the multicystic right lung and secondary compression of the left lung. The baby had severe respiratory distress at birth, with spontaneous pneumothorax (note right chest drain). CT (**e**) performed on day 3 show a complex, multicystic lesion involving the right upper and middle lobes. The residual pneumothorax (*thick black arrow*) and the inserted chest tube (*thin black arrow*) are clearly identified
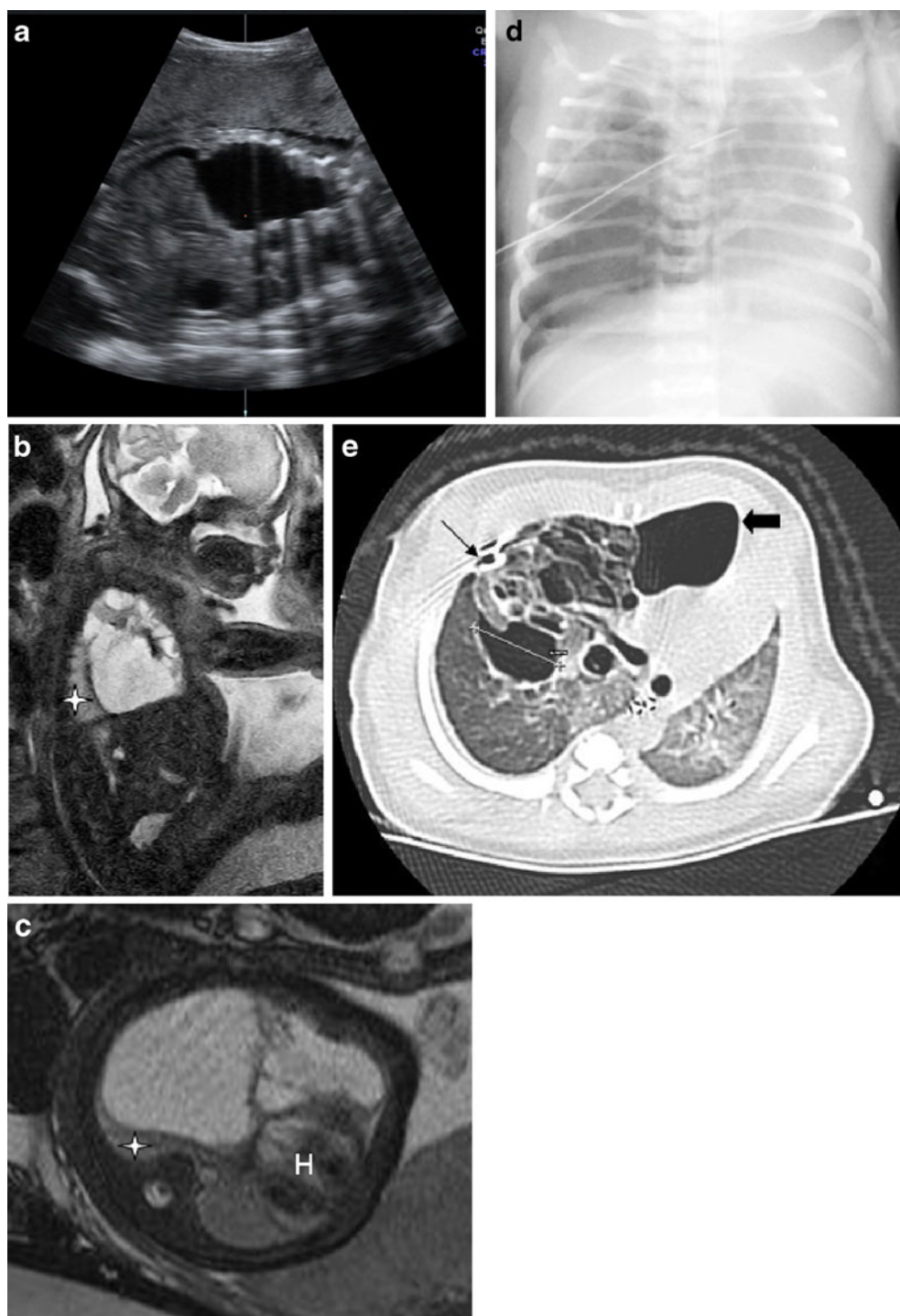

lung may cause mediastinal shift and secondary compression of the contralateral lung (Fig. 3).

In some foetuses with Stocker type II or III lesions, the involved lung is homogeneously hyperechoic and hyperintense compared to normal pulmonary parenchyma. These lesions cannot be differentiated from other CLAs, such as BPS and CLO [13].

CPAM of Stocker type III is debated. Although often considered in the differential diagnosis for a homogeneously hyperintense CLA on imaging, it is rarely confirmed histopathologically. Some consider it a different histopathological entity altogether, often associated with bronchial atresia and poor outcome [9]. Our experience supports this hypothesis, as exemplified in a foetus with proximal atresia

Fig. 4 Small-cystic type congenital pulmonary airway malformation (CPAM). Transverse US of the foetal chest (**a**) at 21 weeks' gestation shows a heterogenous, mostly hyperechoic mass containing several small cysts within the right hemithorax. There is secondary mild mediastinal shift (*H*, heart). T2-HASTE foetal MRI image at 21 weeks' gestation in transverse (**b**) and sagittal (**c**) planes confirms the presence of multiple, similar-sized small cysts in the right lower lobe. Postnatal chest CT performed at 3 months of age (**d**) and 3-D reconstruction image (Volume rendering presets, Chest, Transparent lung, version 2006; Advantage Workstation, General Electric, Milwaukee, WI, USA) (**e**) show the multiple pulmonary cysts and permit re-evaluation of the extension of the lesion, which now seems limited to the apical and posterobasal segments of the right lower lobe
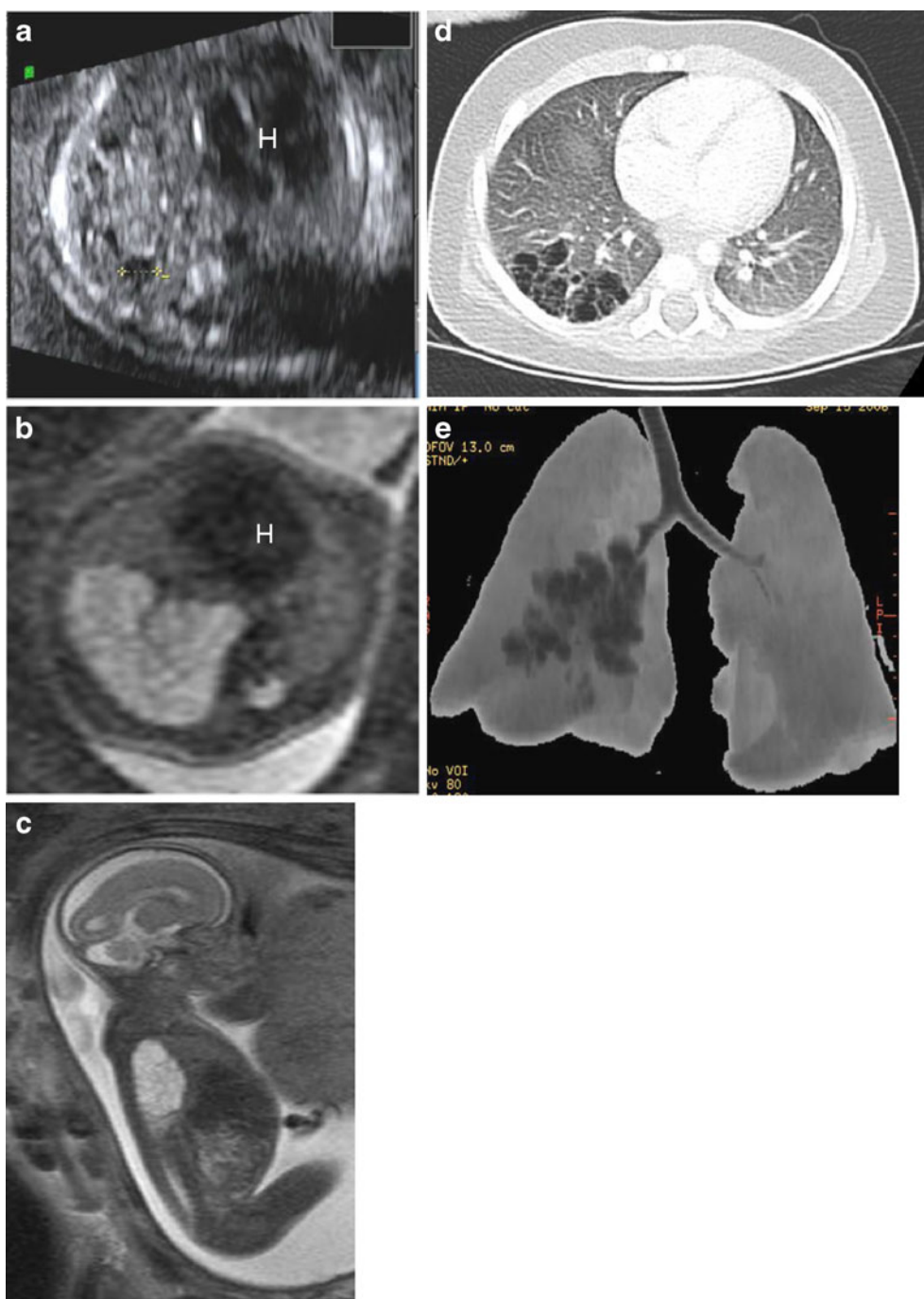
of the right upper lobe bronchus, histologically proven CPAM type III, mass effect, secondary severe hypoplasia of the contralateral lung and a fatal outcome (Fig. 6).

The outcome of CPAM is unpredictable, but a characteristic evolution in utero has been observed. Lesions, most commonly diagnosed during the second trimester, undergo some increase in volume between 20 and 25 weeks' gestation, stabilising in volume toward the end of the second trimester [14]. Subsequent regression has been observed in 20–50% during mid-third trimester, usually at 29–34 weeks' gestation

[4, 14]. Nevertheless, complete involution is extremely rare, so small residual lesions are invariable observed in late gestational MRI and postnatally.

Because of the great variability of lesions and their potential regression in utero, morphological description with foetal US and MRI seems to be the most useful way to characterize lesions. Epelman et al. [15] have recently recommended a description that includes anatomical location, relationship with the bronchial tree, number of cysts and the size of the largest cyst, among other parameters. In

our opinion, this description is practical and transmits the relevant information to the medical team in a comprehensible way.

Bronchopulmonary sequestration

These masses contain nonfunctional lung tissue lacking a normal communication with the tracheobronchial tree. BPS can be extra- or intralobar, with extralobar lesions presenting a separate pleural investment. Both variants have systemic arterial supply (distal thoracic or proximal abdominal aorta or one of its major branches). Venous drainage is via the pulmonary veins for the intralobar and systemic veins (azygos or inferior vena cava) for the extralobar type. These lesions are systemic arteriovenous malformations and may cause cardiovascular symptoms if hemodynamically significant [2].

Extralobar sequestration account for 25% of CLAs (Fig. 5) and may be associated with other congenital systemic anomalies, such as congenital diaphragmatic hernia or cardiac abnormalities. This form may involve in utero. The lesion is usually located at the left costophrenic angle, inferior to the lung, or even within or below the diaphragm. During pregnancy, the differential diagnosis of BPS in the left subphrenic location includes neuroblastoma, adrenal hemorrhage and other primary abdominal abnormalities.

Intralobar sequestration (accounting for around 75%) is usually embedded in a normal lobe [13] (Figs. 5, 7). It is increasingly identified at prenatal US. Langston [16] recently suggested that it is a bronchial atresia with systemic vascular supply [16].

At US, BPS is seen as a hyperechoic, relatively homogeneous mass [1, 10, 12] (Fig. 5). On MRI, it is typically well-defined with uniform high signal intensity compared to normal lung on T2-weighted imaging. The diagnosis is verified with color Doppler (and sometimes with MRI) by the presence of an abnormal vascular supply arising from the aorta or its major branches (Fig. 5) [11, 12]. If the vascular supply is not recognized, BPS is indistinguishable from other congenital lung abnormalities, such as CPAM, bronchial atresia and CLO [12, 17].

Bronchial atresia

This is a rare anomaly characterized by obliteration of a segmental or subsegmental bronchus near its origin, with normally developed distal structures. The apical and the posterior segments of the left upper lobe are most frequently involved. The bronchial obstruction causes accumulation of the foetal lung fluid secreted by the distal alveoli, with dilatation of the bronchi (bronchocele) and pulmonary expansion distal to the obstruction. Recent studies have
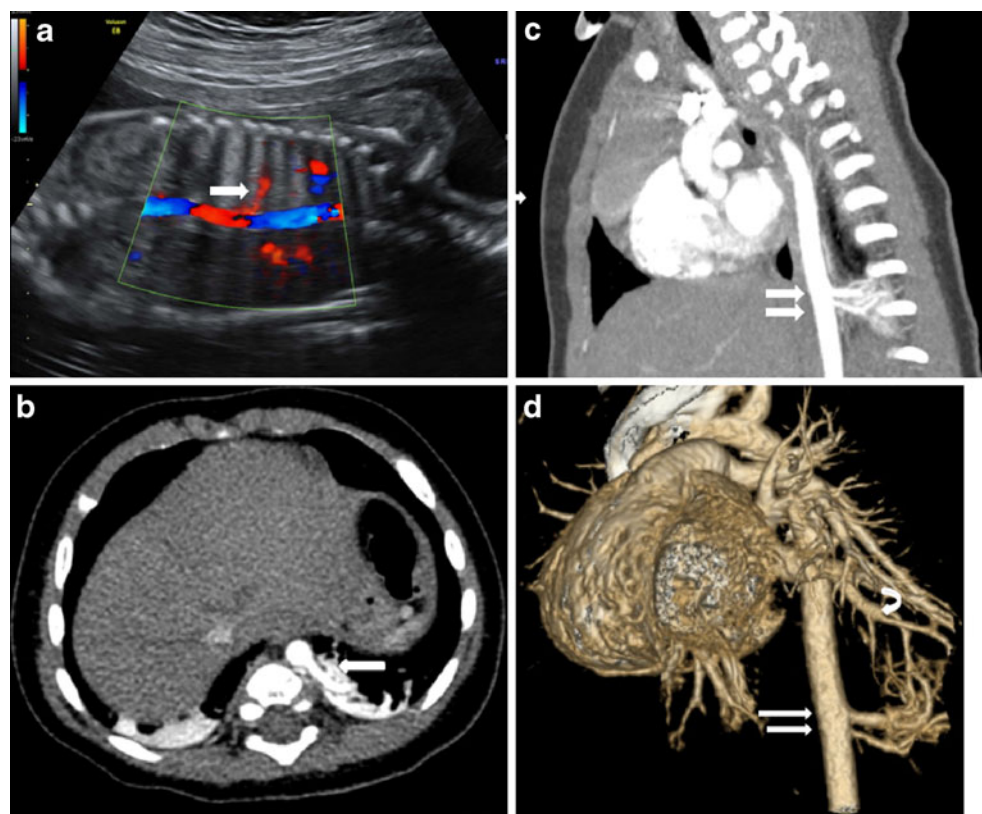

Fig. 5 Intralobar sequestration. Coronal US/color Doppler image (a) of the foetal chest at week 21 clearly demonstrates the abnormal arterial supply to the left lung base (arrow), arising from the distal thoracic aorta. Because of these convincing findings, foetal MRI was not performed. Transverse (b) contrast-enhanced chest CT at 3 months of age confirms the abnormal arterial vascular supply to the left posterobasal segment. Sagittal (c) and surface rendering (d) reconstructions of the same CT data show that there are in fact two abnormal arteries (white arrows) with significant diameter compared to the aorta and show the venous drainage of the lesion via the pulmonary veins (curved arrow)

demonstrated a strong association between bronchial atresia and other CLAs, including intralobar BPS and CPAM, suggesting a common embryological origin [9, 16, 18].

Diagnosis of isolated bronchial atresia has increased in recent years, but its prenatal characterization remains difficult. Although both US and MRI provide good visualization of the trachea and the main bronchi, segmental and subsegmental bronchi are usually not well observed. Prenatally, the

lung (segment or subsegment) involved is expanded, has increased echogenicity and returns high signal on T2-weighted MRI (Fig. 6). In the case of proximal bronchial obstruction, US and MRI may identify the central dilated bronchus or bronchocele (Fig. 6). After birth, CT may identify both the mucus-filled bronchus and the distal surrounding air-trapping that is secondary to collateral ventilation [1, 15].

Fig. 6 Bronchial atresia. Transverse US (a) and transverse (b) and coronal (c) balanced steady-state free precession MRI of the foetal chest at 23 weeks' gestation show a hyperinflated, homogeneously hyperechogenic and hyperintense right lung (star) occupying the majority of the thorax and causing a significant mediastinal shift, with displacement of the heart (H). The left lung is not visualized. Observe the central dilated tubular structure (arrow), which corresponds to the dilated right upper lobe bronchus (bronchocele), distal to the atretic segment. Note also the significant ascites in c. The pregnancy was terminated in week 24. Macroscopic view of the opened thorax at postmortem (d) confirms the enormous expansion of the right upper lobe and secondary severe compression of the contralateral and the remaining ipsilateral lung. The cut surface of the right lung specimen (e) shows the dilated distal bronchus (arrow) and the regional overexpansion of the lung parenchyma. Postmortem confirmed the proximal interruption of the right upper lobe bronchus, consistent with bronchial atresia associated with congenital pulmonary airway malformation Stocker type III
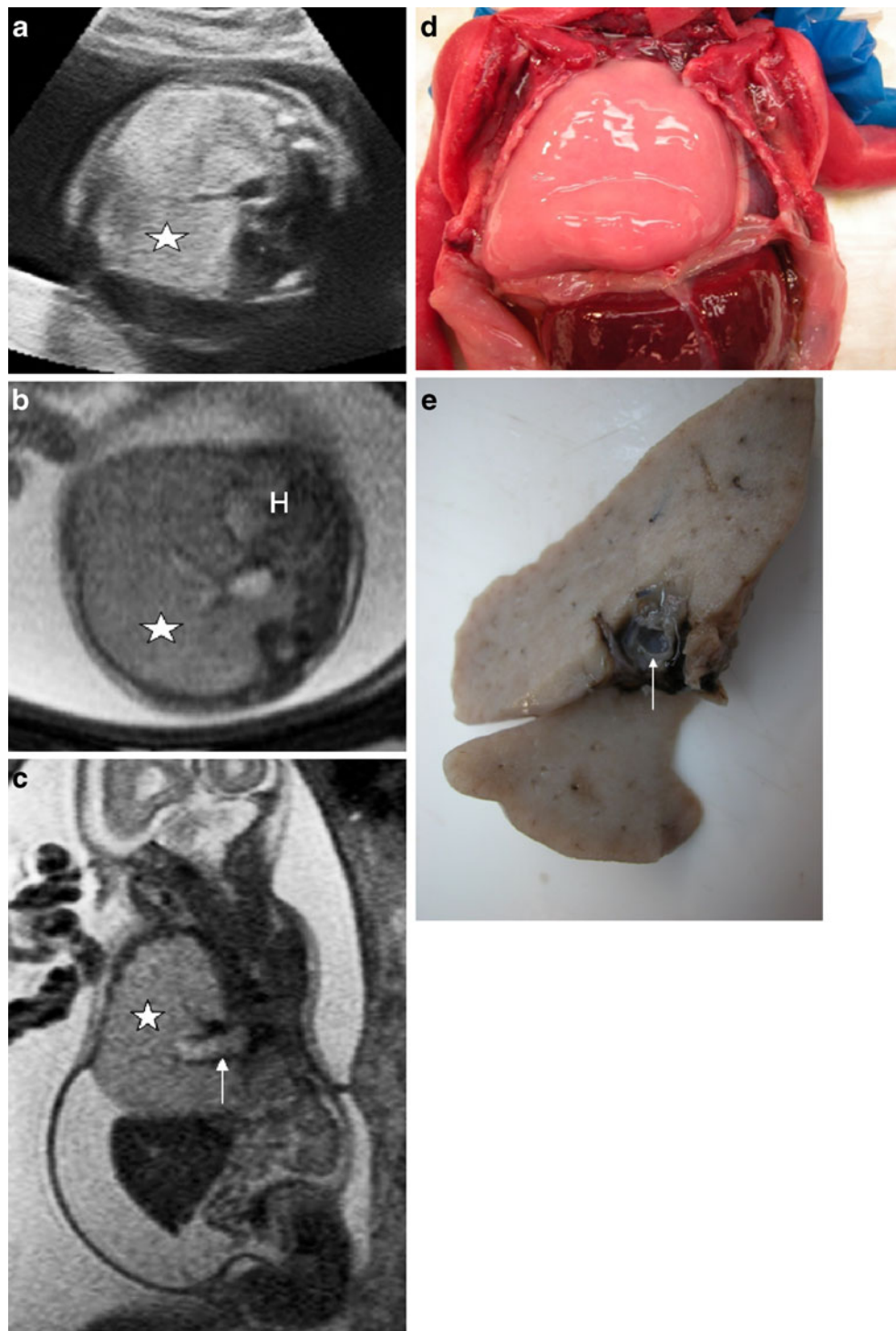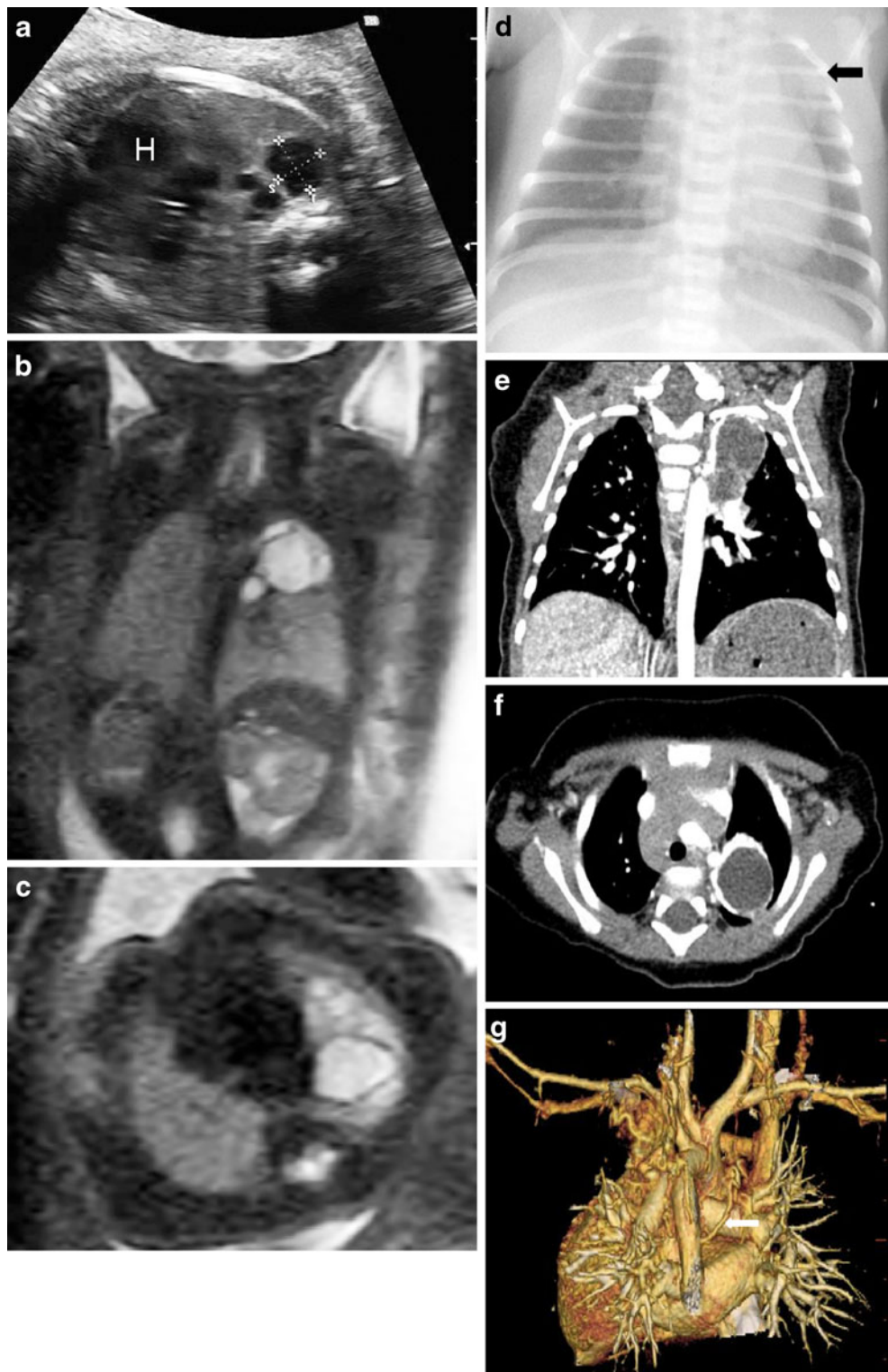
Bronchogenic cysts

These account for 11–18% of mediastinal masses in infants and children and for 40–50% of congenital intrathoracic cysts [8]. They arise from abnormal branching of the

tracheobronchial tree and are typically located near the carina (70%), but may be found paratracheally, in the hila or even within the lung [1]. The cysts are lined with ciliated respiratory columnar epithelium and filled with mucinous material. Bronchial wall structures (e.g., smooth muscle and

Fig. 7 Hybrid lesion: left small-cystic type congenital pulmonary airway malformation (CPAM), bronchogenic cyst and right intralobar bronchopulmonary sequestration. Transverse US (**a**) coronal (**b**) and transverse (**c**) T2-HASTE MRI of the foetal chest at 27 weeks' gestation show a multilobulated, homogeneous hyperechoic and hyperintense multicystic lesion at the apex of the left lung, initially considered a large-cystic type CPAM. **d** Neonatal chest radiograph demonstrates limited aeration of the left upper lobe (*arrow*). Coronal reconstruction (**e**) and transverse section (**f**) from a contrast-enhanced chest CT scan at 6 months of age confirm the fluid-filled mass in the left upper lobe, with an abnormal arterial supply, arising from the left pulmonary artery (not from the thoracic aorta, as is the rule in sequestrations). Surface rendering of the same CT (**g**) reveals an additional unsuspected, right anomalous artery (*arrow*) arising from the distal thoracic aorta and feeding a normal right lower lobe with a normal bronchial tree. This may be considered a variant of a intralobar sequestration (*white arrow*). After segmentectomy of the upper left lobe, specimen showed a complex lesion, with histological characteristics of both bronchogenic cyst and macrocystic CPAM

cartilage) are usually identified. The differential diagnosis includes oesophageal duplication cysts and neurenteric cysts.

At prenatal US, bronchogenic cysts are usually anechoic, uni- or bilocular well-defined masses in the middle mediastinum or in the perihilar regions. At foetal MRI, they have homogeneous high signal intensity on T2-weighted images and low signal intensity on T1-weighted images (Fig. 7). Occasionally, they may cause secondary bronchial compression that causes morphological changes in the lung distal to the obstruction: increase of volume and retention of foetal lung fluid. The retained fluid is homogeneously hyperechoic and is hyperintense on T2-

weighted MRI [12]. In case of bronchial obstruction, the differential diagnosis includes bronchial atresia. Intrapulmonary bronchogenic cysts are extremely difficult to recognize prenatally (Fig. 7), and are easily misinterpreted as macrocystic CPAM with a dominant cyst [13].

Congenital lobar overinflation or emphysema

CLO is characterized by progressive postnatal lobar expansion that causes compression of normal lung. It is usually caused by a focal cartilaginous bronchial wall abnormality [1]. The narrowed airway may postnatally exert a one-way valve effect that results in air-trapping of the distal lung [17]. The

Fig. 8 Hybrid lesion: large-cystic type congenital pulmonary airway malformation with dominant cyst and bronchial atresia. Sagittal (a) and coronal (b) balanced steady-state free precession MRI at 27 weeks' gestation show a large, apparently solitary cystic lesion (arrowheads) within the left hemithorax. The remaining left lung has high signal intensity (white arrow) compared with the normal right lung (star), a sign of retention of pulmonary fluid. There is secondary mediastinal shift (H, heart). Chest radiograph (c) at day 3 reveals the huge aerated left lung cyst. Observe the severe mediastinal shift. Contrast-enhanced chest CT performed at 6 months of age (d) demonstrates additional tiny peripherally located cysts (black arrow). The main cyst is next to the airway, causing obstruction of the segmental bronchus and distal segmental overinflation, similar to findings in bronchial atresia. Observe the dilatation of the distal segment bronchus (white arrow)
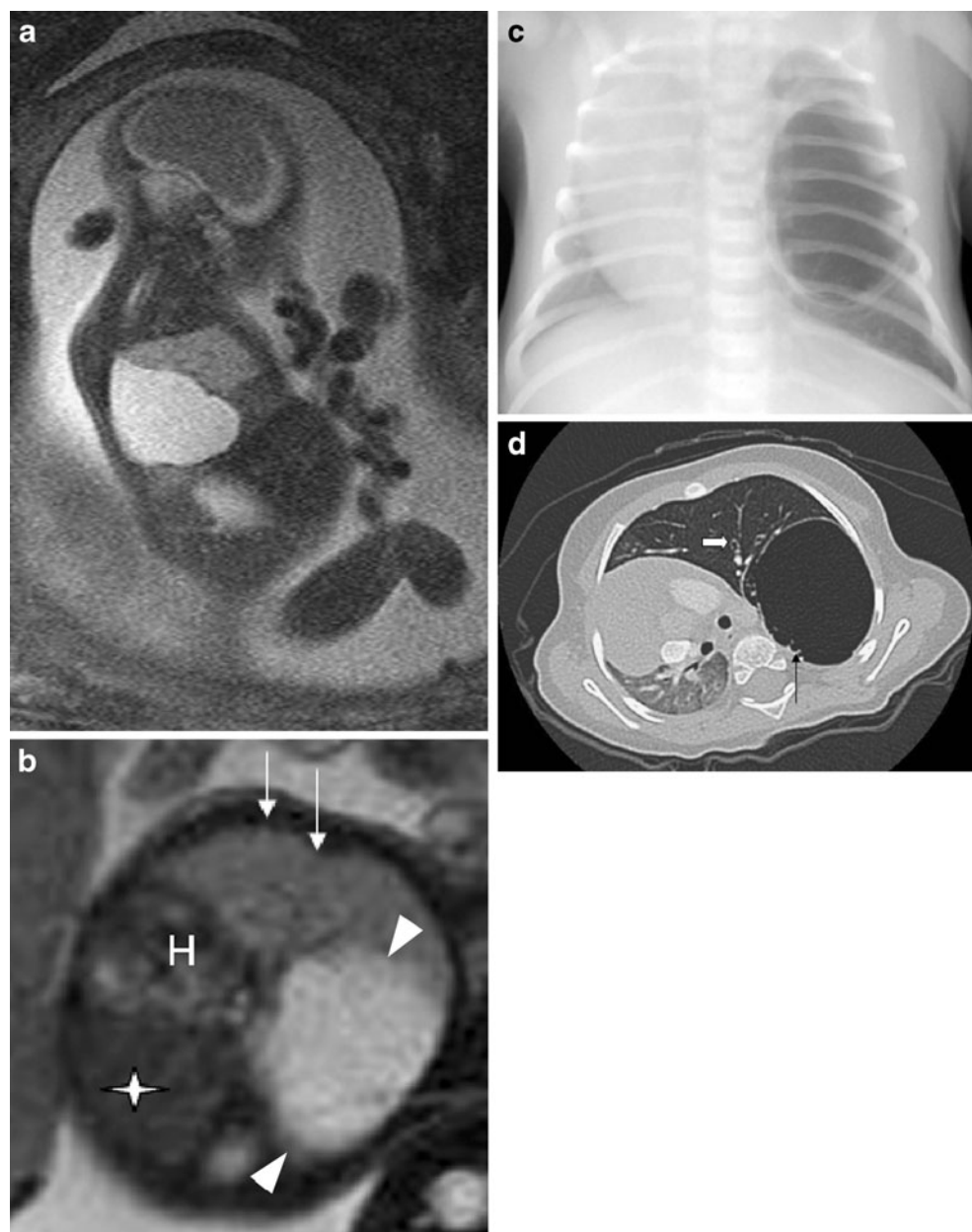
pathogenesis and the dynamism of the lesion, with progressive overinflation of the involved lung, explain the clinical picture: increasing respiratory distress in the neonatal period without any reported prenatal abnormality. Antenatal US and MRI may demonstrate fluid-overloaded, expanded lung tissue with homogeneous hyperechogenicity and MRI hyperintensity and may be difficult to distinguish from other CLA, such as BPS, bronchial atresia and small cystic type CPAM. In most cases, the lung structure is preserved, and stretched vessels are observed [19].

Hybrid lesions

Elements of BPS and CPAM may coexist in hybrid lesions (Figs. 7, 8). Bronchial atresia seems to be present in many cases of BPS and CPAM [8, 16, 18–20]. Indeed, Langston considers these patterns of lung maldevelopment to have a common origin, being the consequence of an in utero airway obstruction and representing a continuous spectrum of anomalies rather than isolated, differentiated lesions. In these cases, complete prenatal characterisation is almost impossible and the suggested prenatal diagnosis would be influenced most by the findings related to the main anomaly. Therefore, postnatal imaging and, in most cases, histopathological evaluation, may be required for a final diagnosis (Figs. 7, 8).

Postnatal diagnosis

In the neonate, CLA may cause a range of clinical pictures, from the asymptomatic child to severe respiratory distress requiring immediate therapy or even an urgent operation. Complete sonographic resolution of a lesion in utero and absence of symptoms at birth are not necessarily proof of complete anatomical normalization. Therefore, all patients with antenatal detected CLA require detailed evaluation with postnatal thoracic imaging [4, 14]. At our institution, children with prenatally detected CLA are investigated postnatally in accordance with a standard protocol that includes plain chest radiographs for all patients at birth. It is known that the progressive postnatal resorption of foetal lung fluid is often associated with significant changes in the morphology of some lesions in the first days of life. For instance, CPAM initially appears (partly) solid and typical air-filled cystic lesions appear only some days after birth. Therefore, repeat chest radiographs during the first neonatal week may be required depending on clinical status.

In the newborn, contrast-enhanced chest CT (CE-CT) is performed only in case of respiratory distress. We do not use CT in asymptomatic children in the immediate postnatal period because of the delayed clearance of the normal foetal pulmonary fluid and the immature renal function [15]. Asymptomatic children undergo CE-CT between 3 and 6 months of life to confirm the prenatal diagnosis, to re-evaluate the extension of the lesion and to determine the origin of the anomalous arterial supply in case of BPS. This informs the discussion about indication for surgical resection.

Resection is the standard intervention for symptomatic lesions, with lobectomy being the usual treatment of choice. The correct care for asymptomatic children is debatable [2]. Although most authors advocate elective resection for CPAM, BPS and bronchogenic cysts because of the risk of complications, some recommend expectant long-term care for asymptomatic children, in particular with CLO. The timing of resection in asymptomatic children is also debated. Most published papers suggest it be performed at 6–12 months of age, attempting to balance the increasing risk of complications and the decreasing potential for pulmonary regeneration with age [2].

Conclusions

CLA is a heterogeneous group of abnormalities with significant overlap of imaging findings. Evidence suggesting a common developmental origin for most CLAs has been growing in recent years. Early airway obstruction in utero is now considered the most probable underlying embryological cause for a wide spectrum of pathologies, with bronchial atresia present in many cases of BPS and CPAM. Although prenatal diagnosis is difficult, an appropriate knowledge of the typical foetal US and MRI findings of the most commonly occurring CLAs permits characterization of a significant number of these lesions in utero. In particular, BPS with evident abnormal vascular supply, large cystic type CPAM and centrally located bronchogenic cysts. In foetal life, US is the most important, and usually the only modality required for lesion characterisation and for identification of unfavorable prognostic factors. Supplementary MRI is useful in selected complicated cases as it allows accurate determination of the location and extension of the lesion and a better assessment of both the normal and abnormal foetal lung, including lung volume measurements.

Different CLAs may have similar prenatal imaging appearances. Complex hybrid lesions are difficult to characterize prenatally and require postnatal imaging or even histopathological examination for a definite diagnosis. Assessment of diagnosis and prognosis based on prenatal imaging therefore needs to be succinct and cautious. Information from prenatal studies needs to be passed on in a comprehensible, descriptive way to facilitate the best pregnancy and postnatal care.

References

1. Berrocal T, Madrid C, Novo S et al (2004) Congenital anomalies of the tracheobronchial tree, lung and mediastinum: embryology, radiology and pathology. Radiographics 24:e17
2. Eber E (2007) Antenatal diagnosis of congenital thoracic malformations: early surgery, late surgery or no surgery. Semi Resp Crit Care Med 28:355–366
3. Vu L, Tsao TJ, Lee H et al (2007) Characteristics of congenital cystic adenomatois malformation associated with noninmune hydrops and outcome. J Pediatr Surg 42:1351–1356
4. Azizkhan RG, Crombleholme TM (2008) Congenital cystic lung disease: contemporary antenatal and postnatal management. Pediatr Surg Int 24:643–657
5. Curran PF, Jelin EB, Rand L et al (2010) Prenatal steroids for microcystic congenital cystic adenomatoid malformation. J Pediatr Surg 45:145–150
6. Stocker JT, Madewell JE, Drake RM (1977) Congenital cystic adenomatoid malformation of the lung. Classification and morphologic spectrum. Hum Pathol 8:155–171
7. Rosado-de-christenson ML, Stocker JT (1991) Congenital cystic adenomatoid malformation. Radiographics 11:865–886
8. Stocker JT (2009) Cystic lung disease in infants and children. Fetal Pediatr Pathol 28:155–184
9. Langston C (2003) New concepts in the pathology of congenital lung malformation. Semin Pediatr Surg 12:17–37
10. Büsing KAK, Schaible T, Neff KW (2006) Fetal MRI. Diagnostic in cases of congenital cystadenomatoid malformation of the lung. Radiologe 46:133–138
11. Williams HJ, Johnson KJ (2002) Imaging of congenital cystic lung lesions. Pediatr Resp Rev 3:120–127
12. Cannie M, Jani J, de Keyzer F et al (2008) Magnetic resonance imaging of the fetal lung: a pictorial essay. Eur Radiol 18:1364–1374
13. Daltro P, Werner H, Gasparetto TD et al (2010) Congenital chest malformations: a multimodality approach with emphasis on fetal MR Imaging. Radiographics 30:385–395
14. Crombleholme TM, Coleman B, Hedrick H et al (2002) Cystic adenomatoid malformation volume ratio predicts outcome in prenatally diagnosed cystic adenomatoid malformation of the lung. J Pediatr Surg 37:331–338
15. Epelman M, Kreiger PA, Servaes S et al (2010) Current imaging of prenatally diagnosed congenital lung lesions. Semin Ultrasound CT MRI 31:141–157
16. Langston C (2003) Intralobar sequestration revisisted. Pediatr Dev Pathol 6:283
17. Biyyam DR, Chapman T, Ferguson MR et al (2010) Congenital lung abnormalities: Embryologic features, prenatal diagnosis and postnatal radiologic-pathologic correlation. Radiographics 30:1721–1738
18. Kunisaki SM, Fauza DO, Nemes LP et al (2006) Bronchial atresia: the hidden pathology within a spectrum of prenatally diagnosed lung masses. J Pediatr Surg 41:61–65
19. Yu-Peng L, Chih-Ping C, Shin-Lin S et al (2010) Fetal cystic lung lesions: evaluation with magnetic resonance imaging. Pediatr Pulmonol 45:592–600
20. Riedlinger WF, Vargas SO, Jennings RW et al (2006) Bronchial atresia is common to extralobar sequestration, intralobar sequestration, congenital cystic adenomatoid malformation and lobar emphysema. Pediatr Dev Pathol 9:361–373